

# Phosducin-Like Protein 3 Is Required for Microtubule-Dependent Steps of Cell Division but Not for Meristem Growth in *Arabidopsis*

M. Mar Castellano and Robert Sablowski<sup>1</sup>

Department of Cell and Developmental Biology, John Innes Centre, Norwich, NR4 7UH, United Kingdom

Given the central role of cell division in meristems, one might expect meristem growth to be regulated by mitotic checkpoints, including checkpoints for correct microtubule function. Here, we studied the role of two close Phosducin-Like Protein 3 homologs from *Arabidopsis thaliana* (PLP3a and PLP3b) in the microtubule assembly pathway and determined the consequences of inhibiting PLP3a and PLP3b expression in the meristem. PLP3 function is essential in *Arabidopsis*: impairing PLP3a and PLP3b expression disrupted microtubule arrays and caused polyploidy, aneuploidy, defective cytokinesis, and disoriented cell growth. Consistent with a role in microtubule formation, PLP3a interacted with  $\beta$ -tubulin in the yeast two-hybrid assay and, when overexpressed, increased resistance to drugs that inhibit tubulin polymerization. Inhibition of PLP3 function targeted to the meristem caused severe mitotic defects, but the cells carried on cycling through DNA replication and abortive cytokinesis. Thus, we showed that PLP3 is involved in microtubule formation in *Arabidopsis* and provided genetic evidence that cell viability and growth in the meristem are not subordinate to successful completion of microtubule-dependent steps of cell division.

## INTRODUCTION

Cell division is a highly regulated process that includes mechanisms to ensure genome integrity, such as the spindle assembly checkpoint, which delays mitosis until all chromosomes are correctly attached to the mitotic spindle (Musacchio and Hardwick, 2002). In animals, cells that cannot satisfy the spindle checkpoint are often eliminated by senescence or apoptosis, reducing the risk of tumorigenesis due to aneuploidy (Rieder and Maiato, 2004; Weaver and Cleveland, 2005). It is not known whether this type of quality control plays a significant role during plant development.

In plants, most cell division occurs in the meristems and in the early stages of organ development (Inze and De Veylder, 2006). At later stages of organ development, growth is based primarily on directional cell expansion, often accompanied by endoreduplication (Sugimoto-Shirasu and Roberts, 2003). Microtubules play key roles in both phases of growth. During cell division, three different microtubule arrays function sequentially: the preprophase band sets the site where a new cell wall is eventually laid, the mitotic spindle drives chromosome segregation, and the phragmoplast organizes the formation of the new cell wall that separates the daughter cells. During interphase, the cortical microtubule array is believed to control the direction of cell

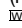
expansion by guiding the pattern of cellulose deposition on the cell wall (Lloyd and Chan, 2004).

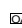
The behavior of microtubules in all these processes is highly dynamic, with constant polymerization and depolymerization of  $\alpha/\beta$ -tubulin heterodimers. To form these heterodimers, both tubulin polypeptides must be properly folded. The initial steps in the folding of cytoskeletal proteins (including actin and tubulins) are guided by a general cytosolic chaperonin called chaperonin containing TCP1 (CCT); a second chaperonin called the prefoldin complex (PFD) is believed to deliver unfolded polypeptides to CCT (Geissler et al., 1998; Vainberg et al., 1998). After the initial folding by CCT,  $\alpha$ - and  $\beta$ -tubulin are passed on to different sets of tubulin-folding cofactors, which eventually converge to assemble the  $\alpha/\beta$  heterodimer (Szymanski, 2002). In *Arabidopsis thaliana*, mutations in several of these tubulin-folding cofactors are embryonic lethal; close examination of the mutant embryos showed that tubulin deficiency led to failure in cell division and in oriented cell expansion (Steinborn et al., 2002).

More recently, a novel step in tubulin folding has been described in yeast. Phosducin-Like Protein 1 (PLP1) was found to interact with CCT and to modulate the efficiency of  $\beta$ -tubulin and actin folding, at an early step distinct from the prefoldin complex (Lacefield and Solomon, 2003; Stirling et al., 2006). Although PLP1 is not an essential gene in yeast, PLP1 homologs (known as PLP3 or PhLP3) are conserved from plants to humans (Blaauw et al., 2003). Data on functional conservation, however, are limited: knockout of PhLP3 did not cause obvious defects in *Dictyostelium discoideum* (Blaauw et al., 2003); mammalian PhLP3 (known as TxnDC9 and APACD) interacted with CCT and interfered with ATP-dependent folding of actin and tubulin (Stirling et al., 2006), but there are no functional data in vivo. In *Caenorhabditis elegans*, RNA interference (RNAi) inhibition of a

<sup>1</sup> Address correspondence to robert.sablowski@bbsrc.ac.uk.

The author responsible for distribution of materials integral to the findings presented in this article in accordance with the policy described in the Instructions for Authors (www.plantcell.org) is: Robert Sablowski (robert.sablowski@bbsrc.ac.uk).

 Online version contains Web-only data.

 Open Access articles can be viewed online without a subscription. www.plantcell.org/cgi/doi/10.1105/tpc.107.057737

*PLP3* homolog (called C05D11.3) caused a reduction in the rate of microtubule growth (Srayko et al., 2005) and resulted in embryo lethality that was attributed to microtubule defects (Ogawa et al., 2004).

Here, we show that *PLP3* function is essential for microtubule-related processes during *Arabidopsis* development: inhibition of the function of two close *PLP3* homologs disrupted microtubule arrays *in vivo* and interfered with microtubule-dependent functions, including nuclear division, cytokinesis, and oriented cell expansion. When inhibition of *PLP3* function was targeted to the shoot meristem, gross defects in cell division were seen but the cells continued to cycle through DNA replication and abortive cytokinesis. Thus, in spite of the central role that cell division plays in meristem function, cell viability and growth in the meristem did not appear to be subordinate to a checkpoint for correct microtubule-dependent functions.

## RESULTS

### *PLP3a* Is Developmentally Regulated

Here, we refer to *Arabidopsis PhLP3* (Blaauw et al., 2003) as *PLP3a* and to a closely related gene, which encodes a protein 90% identical and 97% similar to *PLP3a*, as *PLP3b*.

*PLP3a* initially attracted our attention because microarray experiments indicated that this gene was preferentially expressed in the inflorescence meristem (using whole seedlings as the baseline) and was activated by ectopic expression of the meristem development gene *SHOOT MERISTEMLESS (STM)*, suggesting that *PLP3a* could be relevant to meristem function (C. Woodward and R. Sablowski, unpublished data). RNA *in situ* hybridization confirmed the expression of *PLP3a* in the inflorescence and floral meristems but also showed expression in floral organ primordia and to a lower level throughout the inflorescence tip (Figures 1A and 1B).

For a wider view of *PLP3a* expression, we used reporter genes that contained the complete intergenic region upstream of *PLP3a* and the complete coding sequence and introns, fused with the  $\beta$ -glucuronidase (GUS) or green fluorescent protein (GFP) reporters inserted in frame just before the stop codon. Three independent GUS reporter lines were examined in detail and showed the same pattern. In the inflorescence, GUS expression was detected in the meristem and in young floral buds and subsequently remained strong in parts of the carpels and stamens (Figure 1C). During the vegetative phase, GUS was initially expressed throughout the mature embryo, including the hypocotyl and cotyledons (Figure 1D). In seedlings, expression was highest in the shoot meristem and leaf primordia, in the primary and lateral root meristems, and at the base of the hypocotyls; lower levels were seen in the elongating zone of the root, in the hypocotyls near the shoot apex, and in the vasculature of cotyledons (Figures 1E and 1G); in leaves, the initial expression in the primordia disappeared as the leaves began to expand (Figure 1F). This pattern was consistent with the expression of *PLP3a* in different organs as determined by quantitative RT-PCR (Figure 1H) and reported in publicly available expression array data (<https://www.genevestigator.ethz.ch/at/>).

The two independent GFP reporter lines analyzed showed the same expression pattern as the GUS lines and were used for a more detailed analysis at the cellular level. Optical sections through the inflorescence apex showed GFP throughout the meristem and floral buds (Figure 1I); in the root meristem, GFP was seen in all meristem cells and in the elongation zone (Figure 1J). In both cases, the GFP fusion protein was dispersed in both the cytoplasm and in the nucleus (Figure 1K), similar to the localization reported for *PhLP3* in *C. elegans* (Ogawa et al., 2004).

In summary, expression of *PLP3a* was highest in tissues with active cell division and decreased as cells differentiated but was not exclusively associated with cell division, as it was also seen in the vasculature and in mature reproductive organs.

### Loss of *PLP3* Function Led to Cell Division Defects, Aneuploidy, and Polyploidy

To study the function of *PLP3a*, we initially searched public databases for insertional mutants, but none were available. TILLING (Till et al., 2003) only yielded alleles with amino acid changes (H83N and D93N) that caused no visible phenotypes alone or in combination with the *p1p3b-1* mutation described below. We then inhibited *PLP3a* expression by RNAi, using the widely expressed 35S promoter to direct expression of an RNA hairpin construct matching the *PLP3a* sequence. We recovered three *35S:PLP3a(RNAi)* lines that segregated the construct as single Mendelian loci (to avoid the complication of transcriptional silencing of the transgene) and had reduced levels of *PLP3a* RNA. In seedlings (combined progeny of hemizygous individuals), the levels of *PLP3a* expression ranged from 35 to 72% of the wild-type control, while expression of the closest homolog of *PLP3a* (*PLP3b*) showed only minor changes (Figure 2A). The reduced expression of *PLP3a* in these plants, however, caused no obvious defects.

As *PLP3b* expression overlapped with *PLP3a* (Figure 1H), these genes could be functionally redundant. To test this, we crossed the *35S:PLP3a(RNAi)* lines with a *PLP3b* insertional mutant (*p1p3b-1*) caused by a *Ds* element insertion in the first exon. The *p1p3b-1* mutation abolished expression of *PLP3b* (see Supplemental Figure 1 online), but on its own did not cause any visible phenotypes. However, when each of the three independent *35S:PLP3a(RNAi)* lines was combined with *p1p3b-1* (with both transgene and mutation confirmed by PCR genotyping), a novel phenotype was seen (Figures 2C to 2F). The cotyledons and hypocotyls of *35S:PLP3a(RNAi) p1p3b-1* seedlings appeared rough and deformed, cotyledon number was frequently abnormal (1 to 3), the seedlings failed to produce more than one or two leaves, and in the most severe cases growth of the primary root was also inhibited. A range of phenotypic severity (Figure 2C) was seen in each line, with more severe defects in the lines with the strongest reduction in *PLP3a* expression (lines 1 and 2, Figure 2A). As often seen for RNAi, the penetrance of the abnormal phenotype in populations of *35S:PLP3a(RNAi) p1p3b-1* seedlings was not complete, with the frequency of deformed and arrested seedlings in different lines ranging from 25% (line 1,  $n = 337$ ) to 73% (line 2,  $n = 185$ ). Nevertheless, the fact that these phenotypes were seen only when independent *35S:PLP3a(RNAi)* lines were crossed into the *p1p3b-1*

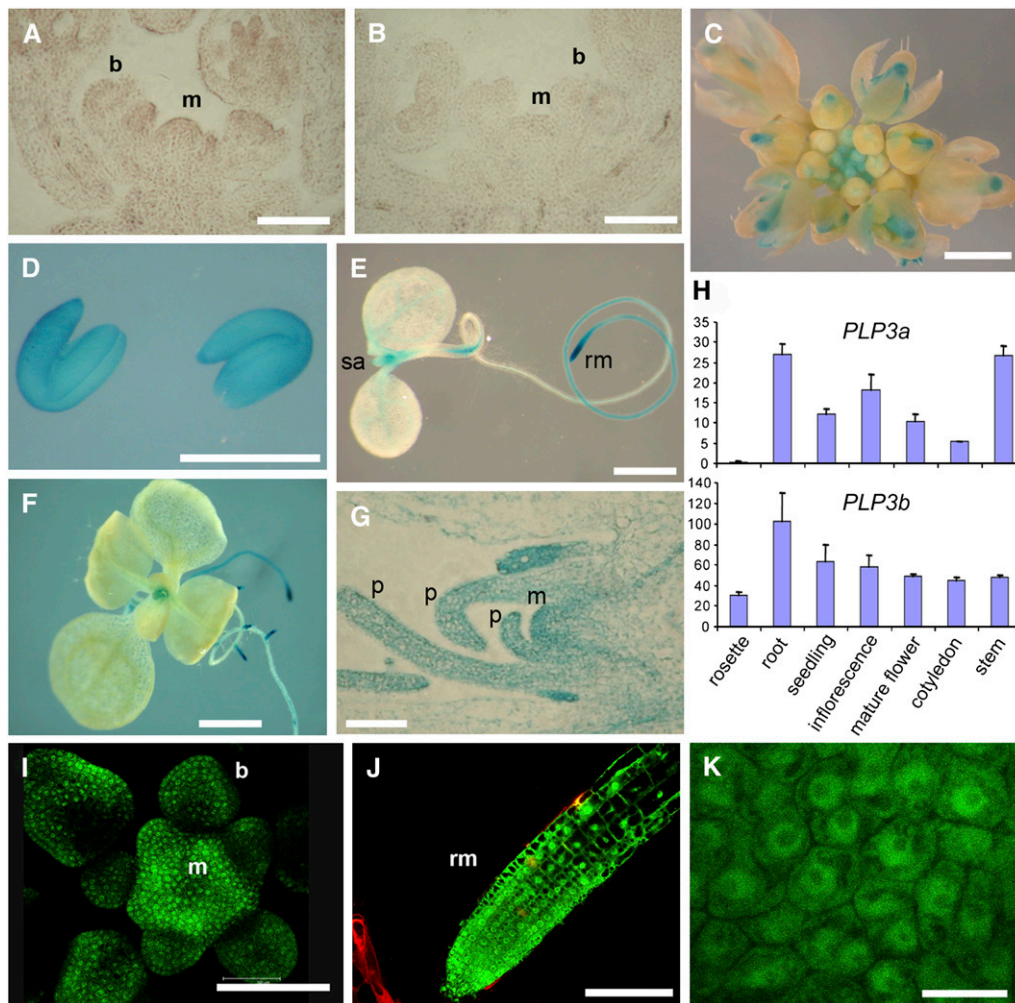


**Figure 1.** PLP3a Expression Pattern.

(A) to (C) Expression in the inflorescence meristem and floral buds.

(A) and (B) In situ hybridization with PLP3a antisense and sense probes, respectively.

(C) Expression of the PLP3a<sub>pro</sub>:PLP3a-GUS reporter in the inflorescence apex.

(D) to (G) Expression in the vegetative phase.

(D) Expression of PLP3a<sub>pro</sub>:PLP3a-GUS in embryos dissected from seeds that had been imbibed for 24 h.

(E) and (F) PLP3a<sub>pro</sub>:PLP3a-GUS expression in seedlings 1 week (E) or 2 weeks (F) after germination.

(G) Section through the shoot apex of a 1-week-old PLP3a<sub>pro</sub>:PLP3a-GUS seedling.

(H) Expression of PLP3a and PLP3b in different tissues measured by quantitative RT-PCR; units on the vertical axis are relative to the level of PLP3a in rosette leaves (which was set to 1). Bars show the average and SD for three independent RNA extractions.

(I) and (J) Optical section through the inflorescence apex (I) and root meristem (J) of a PLP3a<sub>pro</sub>:PLP3a-GFP seedling.

(K) Higher magnification of PLP3a<sub>pro</sub>:PLP3a-GFP expression in the inflorescence meristem.

m, shoot apical meristem; b, floral buds; p, leaf primordia; sa, shoot apex; rm, root meristem. Bars = 100 μm in (A), (B), (G), (I), and (J), 1 mm in (C), (E), and (F), 0.5 mm in (D), and 10 μm in (K).

background confirmed the specificity of RNAi inhibition in these lines (since a knockout of the most closely related gene was still required) and showed that *PLP3b* was indeed able to cover for partial loss of *PLP3a* function during seedling development.

Closer examination of the deformed cotyledons in *35S:PLP3a(RNAi) plp3b-1* plants revealed that they contained enlarged and misshapen cells, sometimes forming a sector

within the cotyledon (Figures 2D to 2F). Partial cell walls (arrows in Figures 2E and 2F) indicated defects in cytokinesis (see also Figure 7H). 4',6-Diamidino-2-phenylindole (DAPI) staining showed that the nuclei of the abnormal cotyledon cells were larger than in the wild type and contained multiple nucleoli, instead of the single nucleolus seen in wild-type cells (cf. insets in Figures 2G and 2H). In the *35S:PLP3a(RNAi) plp3b-1* seedlings, pairs of cells that appeared to derive from a recent mitosis often,

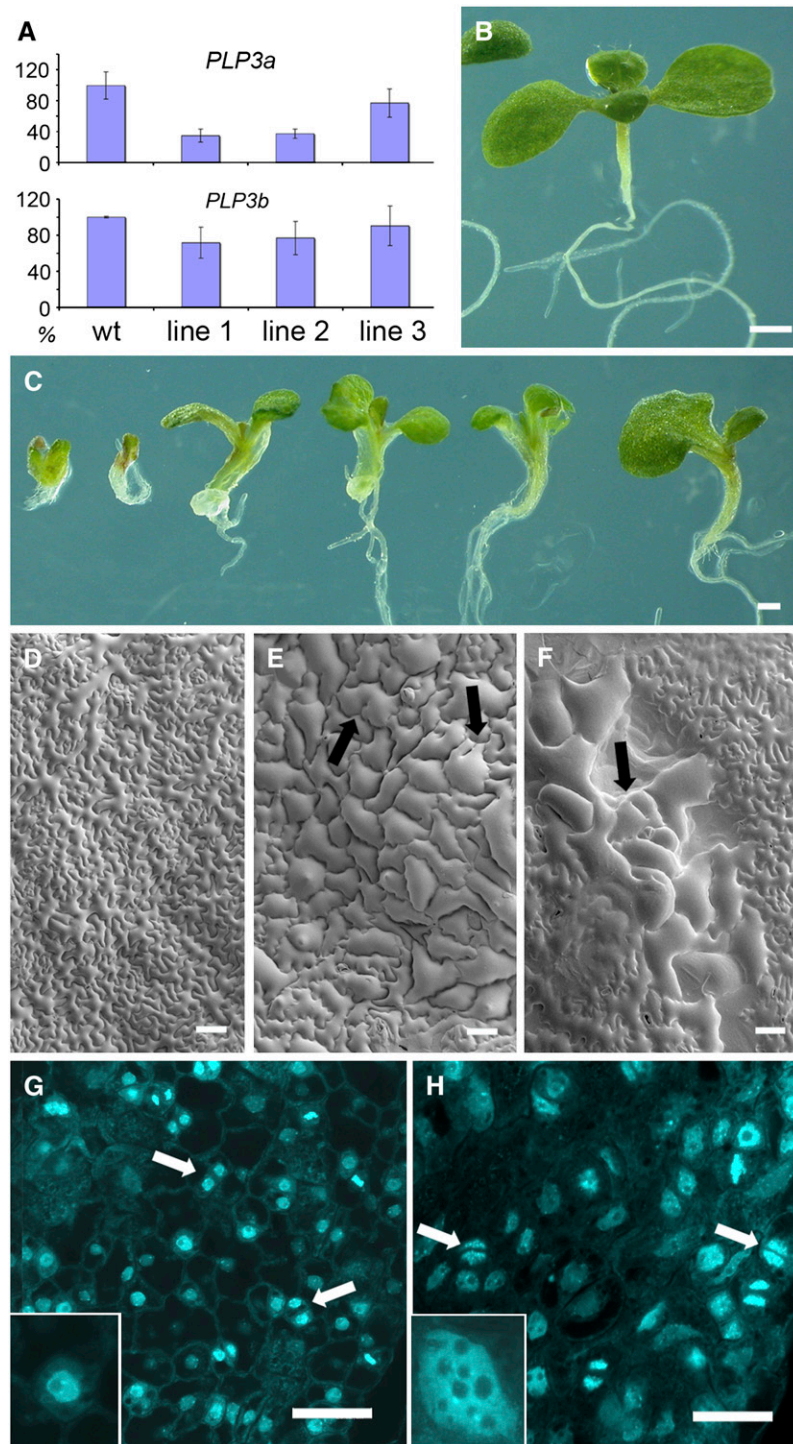


**Figure 2.** Phenotypic Analysis of *PLP3a-35S:RNAi plp3b-1* Plants.

**(A)** Expression of *PLP3a* and *PLP3b* measured by quantitative RT-PCR in 1-week-old seedlings of different 35S:*PLP3a*(*RNAi*) lines; the vertical axis represents expression relative to the wild-type average. Bars show the average and SD for three independent RNA extractions.

**(B)** One-week-old wild-type seedling.

**(C)** One-week-old *PLP3a-35S:RNAi plp3b-1* (line 1) seedlings.

**(D)** to **(F)** Scanning electron micrographs of the cotyledon epidermis of 1-week-old wild-type **(D)**, *PLP3a-35S:RNAi plp3b-1* (line 2) **(E)**, and *PLP3a-35S:RNAi plp3b-1* (line 1) seedlings **(F)**. The arrows indicate partial cell walls.



but not always, had their nuclei very closely juxtaposed (cf. pairs of cells indicated by arrows in Figure 2H with the wild-type controls in 2G).

The large nuclei with extranumerary nucleoli suggested that these cells were polyploid, so we used flow cytometry to measure ploidy in the abnormal seedlings. The *35S:PLP3a(RNAi) p/p3b-1* seedlings had not only increased ploidy but also discrete peaks of nuclei with intermediate levels of DNA content, suggesting aneuploidy (Figure 3).

### Loss of PLP3a/b Function Disrupted Microtubule Arrays

The cellular defects caused by loss of both *PLP3a* and *PLP3b* function suggest a deficiency in microtubule functions, consistent with the proposed role of the closest homolog in yeast (*PLP1*) in an early step of  $\beta$ -tubulin folding (Lacefield and Solomon, 2003). To directly check whether PLP3a and PLP3b are required for microtubule assembly in vivo, we tested whether microtubule arrays were disrupted in the *35S:PLP3a(RNAi) p/p3b-1* seedlings using *Arabidopsis* plants also expressing a fusion between GFP and  $\alpha$ -tubulin (GFP-TUA6; Ueda et al., 1999). GFP-TUA6, *p/p3b-1* seedlings developed normally and showed a normal pattern of cortical microtubule arrays in the cotyledon epidermal cells (Figure 4A). When GFP-TUA6 was crossed into the *35S:PLP3a(RNAi) p/p3b-1* background, the seedlings again developed the enlarged cotyledon cells shown in Figures 2E and 2F. Using the same settings as for Figure 4A, GFP-TUA6 was barely visible in these cells, suggesting that lower levels of GFP-tubulin accumulated. With increased sensitivity, GFP-TUA6 could be detected, but it was not organized in microtubule arrays and sometimes appeared to be inside vesicles (Figures 4C and 4D); this pattern of fluorescence was not detected with the same settings in *35S:PLP3a(RNAi) p/p3b-1* cells lacking GFP-TUA6.

To control for the possibility that loss of *PLP3* function could preferentially affect the accumulation of the GFP-TUA fusion protein, but still leave enough native tubulin to form microtubule arrays that would not be tagged with GFP, we used the microtubule binding MAP4-GFP fusion as an independent microtubule marker (Marc et al., 1998). In agreement with the results using GFP-TUA6, the cotyledon epidermal cells of *35S:PLP3a(RNAi) p/p3b-1* seedlings had only a few faint MAP4-GFP-marked microtubules, contrasting with the wild-type control that showed clear MAP4-GFP-marked microtubule arrays (Figures 4E and 4F).

### Overexpression of PLP3a Increased Resistance to Inhibitors of Microtubule Assembly

The results above showed that PLP3a/PLP3b activity is required for microtubule assembly and for microtubule-dependent pro-

cesses. To determine whether increased *PLP3a* expression would facilitate microtubule function, we tested whether *PLP3a* overexpression would alter the plant's resistance to microtubule poisons.

Plants were generated that expressed a HA-tagged *PLP3a* under the 35S promoter (*35S:HA-PLP3*), and three independent transgenic lines were chosen in which expression of the tagged protein was confirmed by protein gel blotting (Figure 5A). Seedlings of these lines were germinated on media containing propyzamide, oryzalin, or taxol. Both propyzamide and oryzalin are plant-specific microtubule poisons that bind rapidly and reversibly to tubulin subunits. Propyzamide inhibits the assembly of microtubules both in vivo and in vitro (Akashi et al., 1988), whereas oryzalin appears to be incorporated into microtubules and to slow down or inhibit further incorporation of tubulin subunits (Hugdahl and Morejohn, 1993). Taxol, by contrast, stabilizes microtubules in vivo and in vitro (Schiff et al., 1979).

Propyzamide (3  $\mu$ M) and oryzalin (50 nM) had similar effects on wild-type seedlings: root growth was twisted and inhibited by 65 to 70%, and root epidermal cells were grossly enlarged and protruded from the root surface (Figure 5; see Supplemental Figure 2 online). Consistent with its different mode of action, 1  $\mu$ M taxol caused different growth defects: root growth was inhibited to a lesser extent (37%), and root epidermal cells did not swell, but the aerial parts were more strongly affected, showing thickened hypocotyls and inhibited cotyledon expansion (see Supplemental Figure 2 online).

Increased *PLP3a* expression did not affect the way seedlings responded to 1  $\mu$ M taxol (see Supplemental Figure 2 online) but partially suppressed the effects of propyzamide and oryzalin. In the *35S:HA-PLP3a* lines, the inhibition of root elongation by 3  $\mu$ M propyzamide ranged from 41 to 45% (Figure 5B), and the abnormal expansion of epidermal cells was reduced, although twisted root growth was still observed (Figures 5C to 5G). On 50 nM oryzalin, root elongation was rescued in the *35S:HA-PLP3a* lines to a smaller but still significant extent, and swelling of root epidermal cells was visibly reduced (see Supplemental Figure 2 online). In conclusion, overexpression of *PLP3a* partially restored growth in conditions that compromise microtubule assembly, supporting the idea that PLP3 facilitates microtubule formation.

### PLP3a Interacts with $\beta$ -Tubulin in the Yeast Two-Hybrid Assay

A final connection between *PLP3a* and microtubules came from interaction between PLP3a and  $\beta$ -tubulin. A yeast two-hybrid screen using PLP3a as the bait yielded 89 candidate interactors out of 1.2 million clones from an *Arabidopsis* cDNA library. Six of these clones corresponded to three different isoforms of *Arabidopsis*  $\beta$ -tubulin (Figure 6A). In all cases, the clones contained

**Figure 2.** (continued).

(G) and (H) Optical sections through DAPI-stained cotyledon epidermis of 4-d-old wild-type (G) and *PLP3a-35S:RNAi p/p3b-1* (line 1) seedlings (H). The arrows in (H) indicate pairs of nuclei that were closely associated, in comparison with the nuclei of recently divided cells in the wild type (G). The inset in the bottom left corner of (H) shows an individual nucleus containing multiple nucleoli, in contrast with the single nucleolus of the wild-type control (inset in [G], shown at the same magnification).

Bars = 1 mm in (B) and (C), 100  $\mu$ m in (D) to (F), and 25  $\mu$ m in (G) and (H).

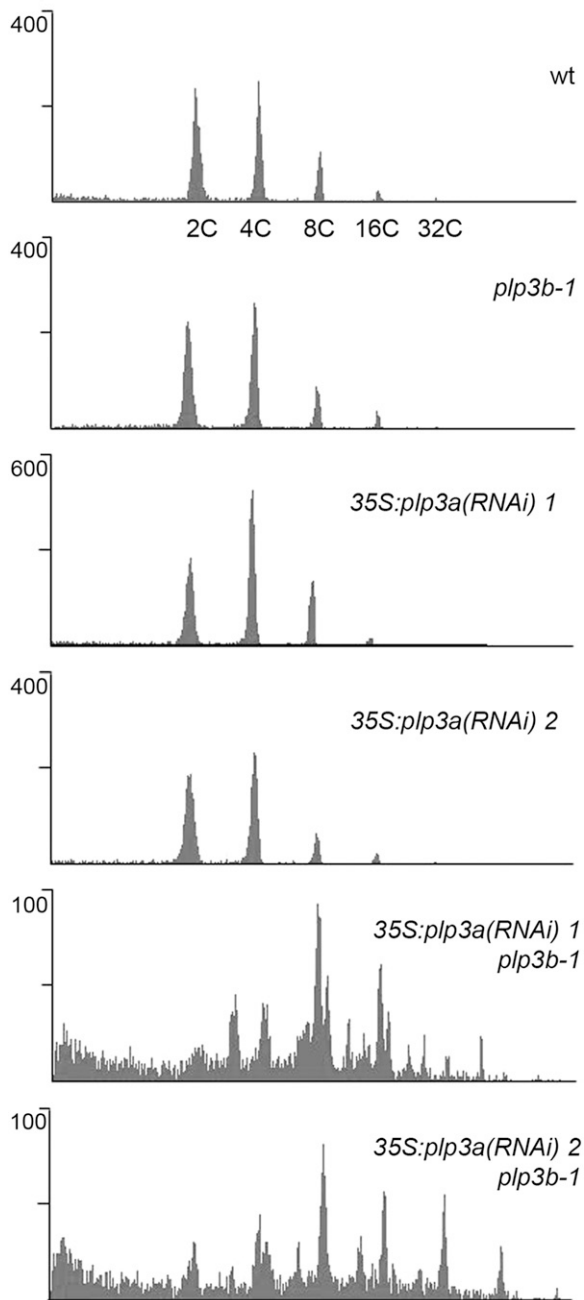


**Figure 3.** Fluorescence-Activated Cell Sorting Analysis of Nuclei from 1-Week-Old Seedlings.

Genotypes are shown on the right. The vertical axis represents the number of nuclei counted; the horizontal axis represents relative fluorescence intensity, with the corresponding ploidy levels indicated for the wild type. Peaks corresponding to the same ploidy level are aligned across all graphs.

fusions between the GAL4 activation domain and the C-terminal region of  $\beta$ -tubulin, suggesting that the interaction with PLP3a occurs within this region (amino acids 300 or 302 to stop for TUB2; 237 or 292 to stop for TUB3; 370 to end for TUB4 and 351 to end for TUB5). Because the various  $\beta$ -tubulin isoforms

show >98% identity over the C-terminal region, only a TUB2 clone was used to confirm the interaction (Figure 6B).

#### Inhibition of PLP3 Function in the Shoot Meristem Disrupted Cell Division but Did Not Prevent Cell Viability and Growth

The results above showed that reduced PLP3 function caused defects in cytokinesis and nuclear division, which are likely due to a general role of PLP3 in microtubule formation. Thus,

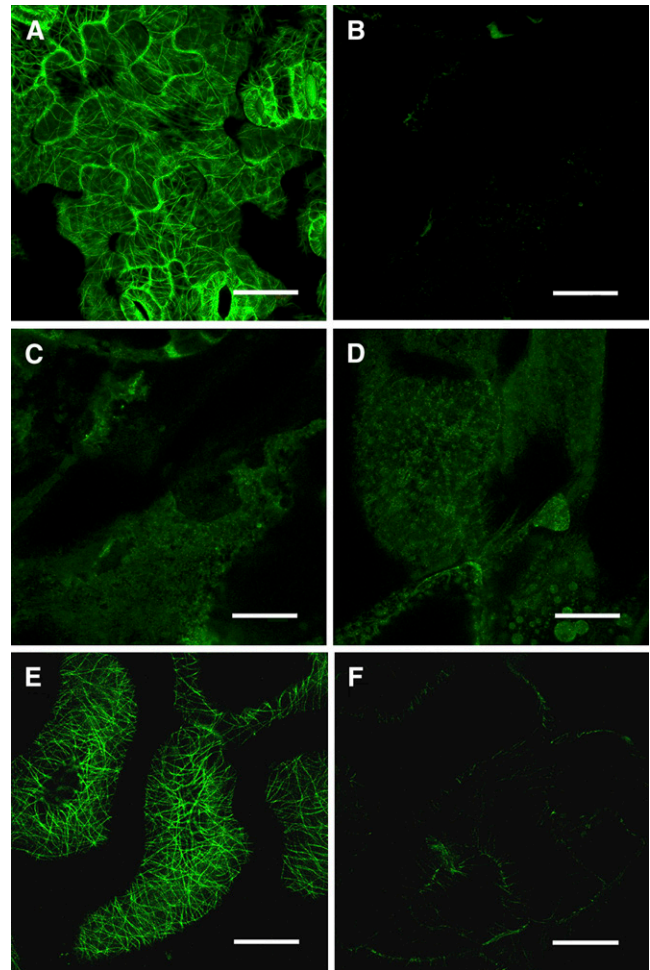


**Figure 4.** Loss of PLP3a/b Function Disrupts Microtubule Arrays.

(A) and (B) Confocal image of cortical microtubule arrays (projections of maximum signal from a stack of 22 0.3- $\mu$ m optical sections) from cotyledon epidermal cells of *plp3b-1*, *GFP-TUA6* seedling (A) or *35S:PLP3a(RNAi) plp3b-1*, *GFP-TUA6* seedling (B).

(C) Image of the same cells as in (B), but with increased gain of GFP signal.

(D) Image of a different set of *35S:PLP3a(RNAi) plp3b-1 GFP-TUA6* cells, collected with the same settings used in (C).

(E) and (F) Confocal image of cortical microtubule arrays (projections of maximum signal from a stack of seven 1.5- $\mu$ m optical sections) from cotyledon epidermal cells of *MAP4-GFP* control plants (E) and *35S:PLP3a(RNAi) plp3b-1 MAP4-GFP* seedling (F).

Bars = 32  $\mu$ m.

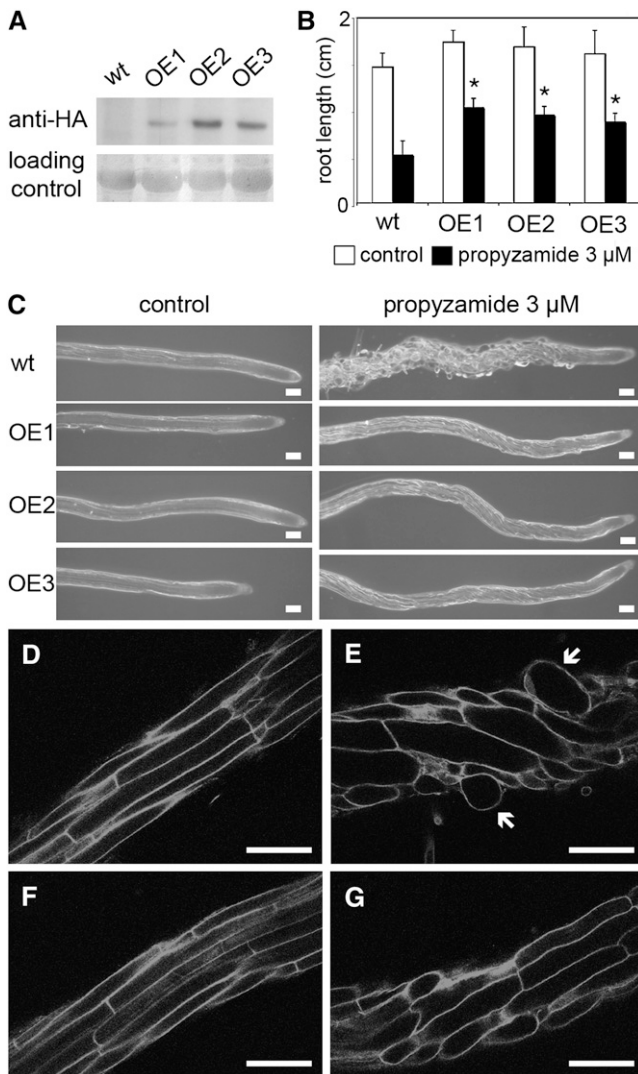


**Figure 5.** Overexpression of HA-PLP3a Increases Resistance to Propyzamide.

**(A)** Protein gel blot showing expression of HA-tagged PLP3a in three different *35S:HA-PLP3a* lines (OE, overexpressor lines 1, 2, or 3). **(B)** Root length in wild-type and in the three *35S:HA-PLP3a* lines shown in **(A)** 1 week after germination on medium containing 3  $\mu$ M propyzamide (stock solution prepared in DMSO) or in control medium with the same amount of DMSO (47 nM). Error bars show SD ( $n = 10$ ). Asterisks indicate significant difference to the propyzamide-treated wild-type control (Student's two-tailed  $t$  test,  $P < 10^{-4}$ ). **(C)** Root morphology of representative plants analyzed in **(B)**; the rough surface of the wild-type root exposed to propyzamide is due to swelling of the epidermal cells, which was suppressed in the overexpressor lines. **(D)** to **(G)** Optical sections through the elongation zone of the wild type **(D)** and **(E)** and *35S:HA-PLP3a* line OE1 **(F)** and **(G)** grown on medium with 0  $\mu$ M **(D)** and **(F)** or 3  $\mu$ M propyzamide **(E)** and **(G)**. Arrows indicate swollen epidermal cells in the wild-type root treated with propyzamide. Bars = 75  $\mu$ m.

inhibition of PLP3 function provided an opportunity to investigate how meristem cells respond to defects in microtubule function that would normally trigger cell cycle arrest or apoptosis in animal cells.

In *35S:PLP3a(RNAi) p/p3b-1* seedlings with a severe phenotype, the shoot apex was disorganized (Figure 2C). This could be due to a requirement of *PLP3a/b* for meristem function, consistent with the expression of *PLP3a* in the meristem and organ primordia, but we could not exclude the possibility that the defective shoot apex was an indirect consequence of earlier defects in embryogenesis. To investigate the role of *PLP3a/b* specifically in the shoot meristem, we generated plants in which the hairpin construct used to make double-stranded RNA matching *PLP3a* was controlled by the *Op* promoter, which is activated by the artificial transcription factor LhG4 (Moore et al., 1998). Two independent *Op:PLP3a(RNAi)* plants were then combined with a transgene in which the meristem-expressed *STM* promoter directs expression of LhG4 (Yanai et al., 2005) in an otherwise wild-type background. Although *STM* is expressed in all shoot meristems, the *STM<sub>pro</sub>:LhG4* line used here is expressed more strongly in the inflorescence and floral meristems, based on activation of an *Op:GFP* reporter (see

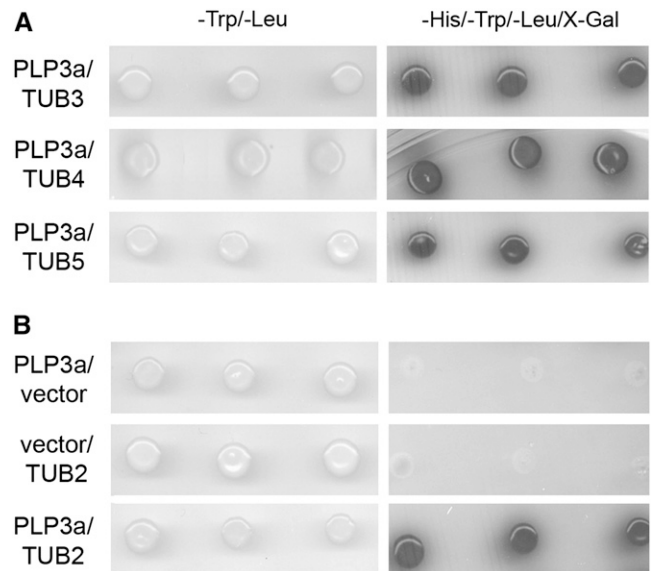


**Figure 6.** PLP3a Interacts with *Arabidopsis*  $\beta$ -Tubulin in Yeast.

**(A)** Growth of clones obtained in a yeast two-hybrid screen, using as the bait the GAL4 DNA binding domain fused to PLP3a. The clones shown contained fusions between different  $\beta$ -tubulin isoforms (TUB3,4,5) and the GAL4 activation domain (AD). The left panels show colonies growing in medium lacking Leu and Trp (to select for both bait and prey) but without testing transactivation; the right panels show colonies grown in medium also lacking His (to test for transactivation of *HIS3*) and containing X-gal (to test for transactivation of the *MEL1* reporter). **(B)** Transactivation of *HIS3* and *MEL1* was confirmed in cells retransformed with the DBD-PLP3a bait and an AD-TUB2 fusion but did not occur in cells that expressed the DBD-PLP3a bait combined with the empty vector expressing the AD only or the empty DNA binding domain vector together with the AD-TUB2 fusion. Left and right panels as in **(A)**.

Supplemental Figure 3 online). For simplicity, the combination of *STM<sub>pro</sub>:Lhg4* and *Op:PLP3a(RNAi)* will be called *STM<sub>pro</sub>:PLP3a(RNAi)*.

As seen for the *35S:PLP3a(RNAi)* plants, *STM<sub>pro</sub>:PLP3a(RNAi)* plants looked normal. By contrast, when two independent *STM<sub>pro</sub>:PLP3a(RNAi)* lines were crossed into the *plp3b-1* background, a striking phenotype was seen in the inflorescence apex. In both the primary and lateral inflorescences, the floral buds at first appeared to develop normally, but a few days after bolting the meristem and young buds were replaced by what superficially looked like disorganized tissue (Figures 7A and 7B). A closer look, however, revealed that the floral buds were still recognizable and were organized in the correct phyllotactic pattern, but contained enormously enlarged cells (Figures 7C and 7D). In the largest of the abnormal buds, these cells measured 50 to 100  $\mu\text{m}$  across, in contrast with the 5 to 10  $\mu\text{m}$  cells seen in buds at approximately the same position in the wild type; roughly, this corresponds to an increase in volume of several-hundred fold. DAPI staining revealed that although greatly enlarged, these cells were not highly vacuolated and retained the high ratio of nuclear-to-cytoplasmic volume that is typical of cells in the meristem and early organ primordia (Figures 7E and 7F). The nuclei, however, were also grossly enlarged and branched; because of their irregular shapes, it was not possible to accurately estimate the DNA content in individual nuclei, but the presence of multiple nucleoli indicated that they were likely polyploid. The irregularly shaped nuclei appeared to weave around partial cell walls, suggesting incomplete cytokinesis. Staining of live tissues with FM4-64 confirmed the presence of cell wall stubs (Figures 7G and 7H), which were seen unambiguously in younger buds, before the cells had enlarged to the same extent as those in Figure 7F. As the buds grew, the enlarged cells did not elongate to the well-defined shapes seen in floral organs of wild-type buds, showing that oriented cell enlargement had also been disrupted.

In summary, loss of *PLP3a/b* function targeted to the shoot meristem caused cellular defects comparable to those seen in the cotyledons of *35S:PLP3(RNAi) plp3b-1* seedlings. Although cell division and cellular organization were severely disrupted, growth of the meristem and floral buds persisted. Partial cell walls indicated that cytokinesis had been initiated in these cells, showing that continued cell growth was not due to a switch to the endoreduplication pathway, but persisted through defective mitosis.

## DISCUSSION

### *Arabidopsis* PLP3a/b Are Required for Microtubule-Dependent Steps of the Cell Cycle

*Arabidopsis* PLP3a/b belong to a family of proteins related to phosducin, which was originally described as a regulator of G-protein signaling in mammals (Bauer et al., 1992). There are three subfamilies of phosducin-like proteins, which had already diverged before the separation between fungi, plants, and mammals (Blaauw et al., 2003). PLP3a/b belong to the phosducin-3 family. The data available in yeast suggest that members of this subfamily are involved in the folding of cytoskeletal proteins. A

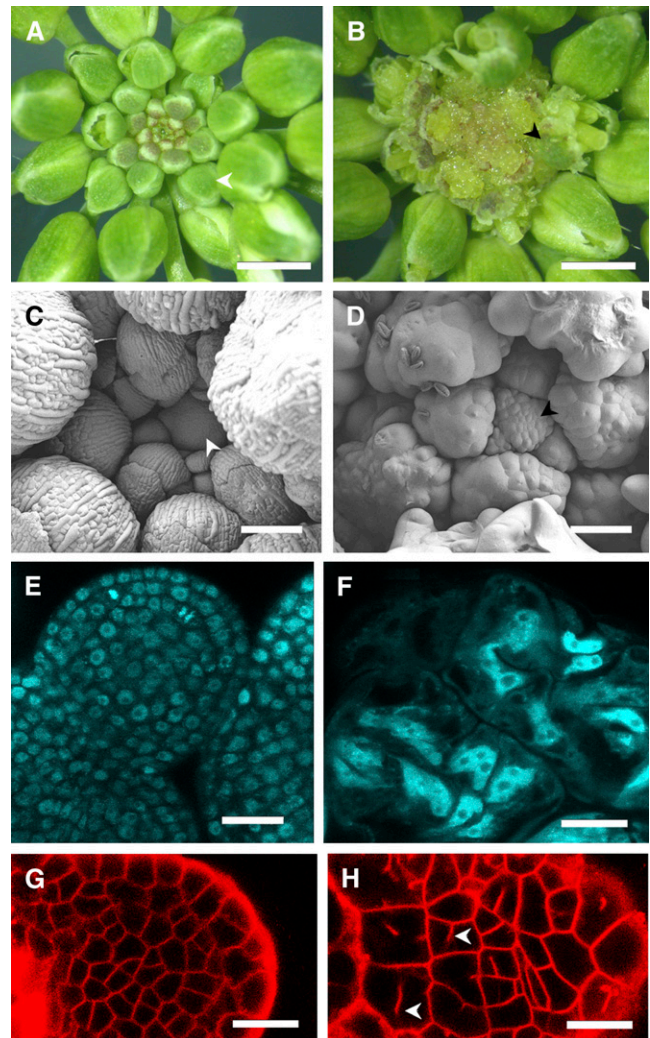


**Figure 7.** Phenotypic Analysis of *plp3b-1*, *STM<sub>pro</sub>:PLP3a(RNAi)* Plants.

(A) and (B) Top view of the inflorescence tips of wild-type (A) and *STM<sub>pro</sub>:PLP3a(RNAi) plp3b-1* plants (B).

(C) and (D) Scanning electron micrographs of wild-type (C) and *STM<sub>pro</sub>:PLP3a(RNAi) plp3b-1* inflorescence tip (D). The arrowheads indicate the inflorescence meristem.

(E) and (F) Optical sections through DAPI-stained floral buds of wild-type (E) and *STM<sub>pro</sub>:PLP3a(RNAi) plp3b-1* plant (F).

(G) and (H) Optical sections through FM4-64-stained floral buds of wild-type (G) and *STM<sub>pro</sub>:PLP3a(RNAi) plp3b-1* plants (H). The arrowheads in (H) indicate partial cell walls.

Bars = 1 mm in (A) and (B), 100  $\mu\text{m}$  in (C) and (D), 20  $\mu\text{m}$  in (E) and (F), and 12.5  $\mu\text{m}$  in (G) and (H).

mutation in *PLP1* (encoding the only member of the phosducin-3 family in yeast) was isolated due to its ability to suppress the toxic effects of excess  $\beta$ -tubulin (Lacefield and Solomon, 2003), although loss of *PLP1* function on its own caused no detectable defects (Flanary et al., 2000). The *plp1 $\Delta$*  mutant did not affect the levels of  $\beta$ -tubulin expression but reduced its ability to form tubulin dimers (Lacefield and Solomon, 2003; Stirling et al.,



2006). Consistent with the model that PLP1 participates in an early step of  $\beta$ -tubulin folding and in parallel with prefoldin, *plp1 $\Delta$*  interacted synergistically with mutants in any of five prefoldin subunits (Tong et al., 2004).

Genes encoding phosducin-3 proteins have been less well characterized in other eukaryotes. No in vivo functional data are available from mammals and *Drosophila melanogaster*. Knock-out of *PhLP3* in *D. discoideum* caused no visible phenotypes (Blaauw et al., 2003). In *C. elegans*, *C05D11.3* has been identified in a systematic RNAi screen for embryo lethality as belonging to the same phenotypic class (exhibiting defects in pronuclear migration, mitotic spindle small or absent) as five other genes, two of which encoded  $\beta$ -tubulin (Gonczy et al., 2000). Consistent with a role in tubulin folding, RNAi of *C05D11.3* decreased the rate of microtubule growth in these embryos, as did RNAi of CCT and prefoldin subunits (Srayko et al., 2005). A more detailed developmental analysis showed that the embryo lethality was accompanied by defects in nuclear-centrosome rotation and pronuclear migration, both of which require microtubules, formation of a short, defective mitotic spindle, failure in chromosome segregation, and aborted cytokinesis (Ogawa et al., 2004). In spite of these defects in cell division, DNA replication seemed to proceed for multiple rounds, similar to our own results in *Arabidopsis*.

We show that differently from yeast and *D. discoideum* but similarly to *C. elegans*, phosducin-3 homologs are essential in *Arabidopsis*. The phenotypes caused by loss of *PLP3a/b* function suggest defects in at least three microtubule-dependent processes. First, aneuploidy and polyploidy suggest a failure in chromosome segregation due to a defective mitotic spindle. Our attempts to directly image mitotic spindles in cells with inhibited *PLP3a/b* function were not successful, but the closely juxtaposed nuclei seen in recently divided cells (Figure 2H) are noteworthy because they might result from abnormally short spindles, which have been reported for yeast and *C. elegans* with reduced *PLP3* function (Ogawa et al., 2004; Srayko et al., 2005; Lacefield et al., 2006). Second, partial cell walls are typical of mutations in genes required for cytokinesis, some of which are directly involved in regulating microtubule behavior, such as *HINKEL* and *PLEIADE* (Strompen et al., 2002; Muller et al., 2004), and have been proposed to regulate genes required for microtubule functions, in the case of *TSO1* (Hauser et al., 2000; Song et al., 2000). It must be noted that polyploidy might also result from nuclear fusion after failed cytokinesis. This is seen in the *knolle* and *keule* mutants (Waizenegger et al., 2000; Assaad et al., 2001; Sollner et al., 2002), although inhibition of cytokinesis by a dominant-negative version of the NPK1 kinase resulted in multinucleate cells instead of nuclear fusion (Nishihama et al., 2001, 2002). In our case, the fact that aneuploidy was also observed suggests that at least some of the nuclear division defects seen in the *PLP3a/b* RNAi lines were not an indirect consequence of failed cytokinesis. The third microtubule-related defect caused by inhibition of *PLP3a/b* was aberrant cell expansion, which requires the cortical microtubule array (Lloyd and Chan, 2004). In the case of the cortical arrays, we have been able to use the microtubule markers GFP-TUA6 and MAP4-GFP to show directly that *PLP3a/b* are involved in microtubule formation. In addition to the loss-of-function data, the increased resistance to

microtubule poisons caused by overexpression of *PLP3a* also indicated that this protein supports microtubule-dependent functions.

Although most of the data in other organisms also indicates that *PLP3* homologs are involved in microtubule formation, mammalian PhLP3 also affected folding of actin in vitro and the yeast *plp1 $\Delta$*  mutation enhanced actin polymerization defects seen in the *pac10 $\Delta$*  mutant, which affects a PFD subunit (Stirling et al., 2006). Although we have not addressed here whether *Arabidopsis* *PLP3* might also play a role in actin folding, the cellular phenotype caused by inhibiting *PLP3* function did not suggest defects in actin filaments because the actin cytoskeleton participates in general cell growth (Steinborn et al., 2002), which continued in the plants with low *PLP3a/b* function, while microtubules are required for directional growth, which was disrupted in these plants. Since our RNAi lines did not completely abolish *PLP3a* expression, we cannot exclude that *PLP3a/b* could also play a role in actin folding, but even if this were the case, our data suggest that the levels of *PLP3* function are more critical to support the assembly of microtubule arrays than the formation of the actin cytoskeleton.

Given the proposed role of the yeast homolog (*PLP1*) in  $\beta$ -tubulin folding, it is reasonable to propose that *PLP3a/b* supports microtubule functions through the production of functional tubulin. Accordingly, *PLP3a* interacted with  $\beta$ -tubulin in yeast two-hybrid assays. At the same time, the localization of *PLP3a*-GFP, which was similar to that reported for the *C. elegans* homolog (Ogawa et al., 2004), was not indicative of association with microtubules, suggesting that the interaction with  $\beta$ -tubulin occurs before microtubule assembly. A role of *PLP3a/b* in tubulin folding would also be consistent with the similarity between the cellular phenotype caused by loss of *PLP3a/b* function and by mutations in genes of the *PILZ* group, which encode tubulin-folding cofactors in *Arabidopsis* (Steinborn et al., 2002). The embryos of these mutants have grossly enlarged cells with one or more large nuclei and cell wall stubs caused by a failure in cytokinesis (Steinborn et al., 2002). In the *Arabidopsis* endosperm, mutation in tubulin folding cofactor D (*titan1* mutant) also results in giant nuclei due to repeated DNA replication without nuclear division (Tzafrir et al., 2002). Although all strong loss-of-function alleles of these genes are embryo lethal, weaker alleles such as *por-T1* and *kis-T1* do develop beyond embryogenesis and show seedling defects very similar to those reported here for *35S:PLP3a(RNAi) plp3b-1* plants. In these mutants, however, no meristem defects have been described (Kirik et al., 2002a, 2002b).

#### Disruption of Microtubule-Dependent Steps of Cell Division Does Not Prevent Cell Viability and Growth in the Shoot Meristem

The cellular phenotypes and the disruption of cortical arrays caused by loss of *PLP3* function, the interaction between *PLP3* and tubulin, and the widely conserved role of *PLP3* homologs in tubulin folding all indicated that *Arabidopsis* *PLP3* plays a general role in microtubule formation. We then used localized loss of *PLP3* function as a genetic tool to investigate the response of meristem cells to defective microtubule functions.

As seen in cotyledon cells, loss of *PLP3a/b* function targeted to the inflorescence and floral meristems disrupted cellular processes in which microtubules play a major role, such as nuclear division, cytokinesis, and oriented cell expansion. Thus, the high expression of *PLP3a/b* seen in the meristems is required to support steps of cell division that are known to depend on microtubules. It must be noted, however, that *PLP3a/b* are also expressed in some differentiated tissues, such as vasculature and in reproductive organs, so *PLP3a/b* are also likely to support microtubule-dependent processes that are unrelated to cell division.

In spite of the severe disruption of cell division in *35S:PLP3a* (*RNAi*) *plp3b-1* plants, meristem growth and cell viability persisted. A similar, but milder phenotype has been described for the *ts01* mutant, which affects a nuclear protein that has been proposed to control the transcription of genes required for cell division (Liu et al., 1997; Hauser et al., 1998, 2000; Song et al., 2000). Considering that *TSO1* is expressed in the inflorescence in a pattern similar to that of *PLP3a*, it will be interesting to see whether *PLP3a/b* might be among the targets of *TSO1* during inflorescence development.

The continued growth of the meristem and organ primordia in spite of severe cell division defects has two wider implications. First, it adds support to the idea that the mechanism that promotes growth in the meristem is not subordinate to correct cell division. Meristem growth is tolerant to several types of defects in cell division. The *ton* and *fass* mutants showed that the orientation of cytokinesis is not critical for meristem function and organ growth (Torres-Ruiz and Jurgens, 1994; Traas et al., 1995). Reduction of the cell division rate using a dominant-negative version of CDC2 led to a compensatory increase in cell size (Hemerly et al., 1995). Blocking mitosis with oryzalin did not stop differential cell growth or changes in gene expression related to primordium emergence (Grandjean et al., 2004). Our results provide genetic evidence that meristem growth persists after disruption of microtubule functions, in spite of abortive cell division and a severely disrupted cellular organization.

The apparent tolerance of meristem cells to defective mitosis also has implications for the maintenance of genome stability in plants. In animal cells, microtubule poisons disrupt the mitotic spindle and cause a delay in M-phase; if the cells eventually overcome this delay and exit mitosis without having corrected the spindle defect, they often withdraw permanently from the cell cycle or undergo apoptosis (Rieder and Maiato, 2004; Weaver and Cleveland, 2005). Treatment of the shoot meristem with oryzalin was expected to disrupt the mitotic spindle and cause a similar block in the cell cycle, but surprisingly, the meristem cells appeared to switch to endoreduplication, which does not include M-phase and the associated spindle checkpoint (Grandjean et al., 2004). In our experiments, however, the presence of abortive cytokinesis implied that the cells did not switch to the normal, developmentally programmed endoreduplication cycle (Sugimoto-Shirasu and Roberts, 2003). Given that meristem cells remained viable and carried on cycling in spite of gross defects in nuclear division, it would be expected that milder defects leading to ploidy changes would also be tolerated, and in fact this phenomenon has been used for decades as the basis for selecting polyploid varieties by treatment with colchicin or

oryzalin. The apparent lack of an effective quality control mechanism to eliminate meristem cells at risk of ploidy defects may have contributed to the disproportionate role that polyploidization has had in plant evolution (Adams and Wendel, 2005).

## METHODS

### Plant Material

*Arabidopsis thaliana* (Landsberg *erecta* [Ler] or Columbia) was grown in vermiculite:soil:sand mix at 18°C, on a 16-h-light/8-h-dark cycle. Plants were transformed by the floral dip method (Clough and Bent, 1998) with the constructs described below, using *Agrobacterium tumefaciens* strain C58C or strain GV3103 RK9 containing pSOUP (for pGREEN derivatives).

The *plp3b-1* mutation (Ler background) has a Ds insertion in the first exon of At5g66410 and was obtained from the CSHL Genetrap collection (<http://genetrap.cshl.org>, line GT9152). The *STM<sub>pro</sub>:LhG4* line (Ler) was a gift from Yuval Esched (Weizmann Institute, Tel Aviv, Israel). *Arabidopsis* lines containing GFP-TUA6 (Ueda et al., 1999) and MAP4-GFP (Marc et al., 1998) were obtained from Clive Lloyd (John Innes Centre); the 35S:ABD2-GFP line (Wang et al., 2004) was provided by Karim Sorefan (John Innes Centre). The transgenes and *plp3b-1* mutation were combined by cross-pollination. Segregation at the *PLP3b* locus was monitored by PCR with primer 5'-TCTCTGGCTATCTTAGAGGGATTTTTG-3' combined with 5'-ACCCGACCGGATCGTATCGGT-3' (for *plp3b-1*) or with 5'-TTCTTGACCAGAAGATTCTCCAGC-3' (for the wild type). Transgenes were genotyped with primer 5'-CTCCTCCTCTGCTAACGTAAGCCTC-3' combined with 5'-GTGAAATCGTCCTTGGTCCCAGATCC-3' (*PLP1a-35S:RNAi*) or 5'-GAGATAGATTTGTAGAGAGAGACTGGTGATT-3' (*PLP1a-Op:RNAi*).

### DNA Constructs

To generate *PLP3a* reporter fusions, a genomic fragment from nucleotide -641 (relative to the start codon) to the end of the coding sequence was amplified from Ler DNA using the primers (5'-AAAACCCGGGAATCGAAAATATACTTCTTTAAC-3') and (5'-TTTACCATGGAGTCCAGATCTCTGAAGACCTAAC-3'). This fragment was cloned into pcr2.1-TA (Invitrogen) and fused in-frame with the *NcoI* site containing the start codons of GFP or GUS. These translational fusions were subcloned into the binary vector pGreen0229 (Hellens et al., 2000) to generate *PLP3a<sub>pro</sub>:PLP3a-GFP* and *PLP3a<sub>pro</sub>:PLP3a-GUS*, respectively.

To create *35S:PLP3a(RNAi)*, which contains the 35S promoter directing expression of inverted repeats of *PLP3a*, the coding sequence for *PLP3a* was amplified from floral cDNA using the primers (5'-ATGGACCCAGATGCAGTCAAATCGACTCTC-3') and (5'-CAACTGCTTGATCAGTCA-GAATC-3') and cloned into pcr2.1-TA (Invitrogen). The *PLP3a* cDNA was subcloned into pENTR4 (Invitrogen) and recombined using the Gateway system (Invitrogen) into pJawohl17-RNAi (gift from Imre Somsich, Max Planck Institute, Koeln, Germany). To create *Op:PLP3a(RNAi)*, the *PLP3a* inverted repeats from *35S:PLP3a(RNAi)* were cloned into the *Sall* site of pW49 (gift from Phil Wigge, John Innes Centre), modified from pU-6Op.Ω (gift from Ian Moore, Oxford University, UK). The resulting *Op:PLP3a(RNAi)* construct contained six copies of the Op sequence and the tobacco mosaic virus Ω leader, upstream of the *PLP3a* inverted repeats, followed by the cauliflower mosaic virus terminator.

To generate *35S:HA-PLP3a*, full-length *PLP3a* cDNA was amplified using the primers (5'-GGGGACCACTTTGTACAAGAAAGCTGGGTCTCAGTCA-GAATCAGAGTCCAGATTTCTTG-3') and (5'-GGGGACAAGTTTGTACAAAAGCAGGCTTGGATCCAGATGCAGTCAAATC-3') and recombined into pDONR201 (Invitrogen), then into pGWB15 (gift from Tsuyoshi Nakagawa, Shimane University, Japan), which allows HA tagging of proteins under the 35S promoter.

## Microscopy Techniques

For RNA in situ hybridization (Gomez-Mena et al., 2005), digoxigenin-labeled riboprobes were used (full-length cDNA for the sense probe and nucleotides 446 to 693 for the antisense probe). Whole-mount GUS detection was performed as previously described (Sieburth and Meyerowitz, 1997); for thin sections, the tissues were treated and sectioned as for the in situ hybridization experiments. For scanning electron microscopy, flowers of 5-week-old plants or cotyledons were mounted on an aluminum stub using O.C.T. compound (BDH Laboratory Supplies). The stub was plunged into liquid nitrogen and transferred onto an ALTO 2500 cryo-transfer system (Gatan) attached to a Zeiss Supra 55 VP FEG scanning electron microscope. Sublimation of surface frost was performed at  $-95^{\circ}\text{C}$  for 3 min before sputter coating the sample with platinum for 2 min at 10 mA,  $-110^{\circ}\text{C}$ , and imaging at  $-130^{\circ}\text{C}$  at 3 kV. Confocal microscopy was performed using a Leica TCS SP2 microscope and the associated software. For imaging nuclei, plant tissues were fixed in PBS containing 4% formaldehyde, washed in PBS, and stained with 1  $\mu\text{g}/\text{mL}$  of DAPI (Sigma-Aldrich). Excitation was set at 405 nm (diode laser) and emission filtered to 420 to 500 nm. For imaging cell walls, live tissues were stained with 50  $\mu\text{g}/\text{mL}$  FM4-64 (Molecular Probes) and imaged with excitation at 488 nm (He laser) and emission filtered to 600 to 660 nm. For GFP imaging, excitation was at 488 nm and emission between 500 and 550 nm; GFP-negative control tissues gave no signal with the settings used. Images were processed (brightness, color balance, and size) with Adobe Photoshop CS2 9.0 (Adobe Systems).

## Quantitative RT-PCR

RNA was extracted from adult *Arabidopsis Ler* plants (rosette leaves, inflorescence, mature flowers, and stem) or from 2-week-old seedlings grown on GM medium (root and cotyledon samples), using TRI reagent (Sigma-Aldrich) according to the manufacturer's instructions. Treatment with 10 units of RNase-free DNase I (Amersham) for 30 min at  $37^{\circ}\text{C}$  was followed by a phenol/chloroform extraction. Total RNA (1.5  $\mu\text{g}$ ) was used for first-strand cDNA synthesis using oligo(dT) primer and the M-MLV reverse transcriptase (Invitrogen). Quantitative RT-PCR was performed using SYBR Green JumpStart (Sigma-Aldrich) in a DNA engine Opticon2 (MJ Research) following the manufacturer's instructions. Values were normalized using adenosine phosphotransferase (*APT1*) as the internal reference. The primers were as follows: for *PLP3a*, 5'-CAGATTTT-GGTGTTAAAAGATGG-3' and 5'-ATCCTTATGGTAGAAATGAC-3'; for *PLP3b*, 5'-TCTCTGGCTATCTTAGAGGGATTTTG-3' and 5'-GTCGCC-TTCGCTAACTTCTCGG-3'; and for *APT1*, 5'-CCTTCCCTTAAGCTCTG and 5'-TCCCAGAATCGCTAAGATTGCC-3'.

## Flow Cytometry

The ploidy level of individual flowers or 3-week-old seedlings was measured by flow cytometry as described (Sugimoto-Shirasu et al., 2002).

## Treatments with Microtubule Poisons

Wild-type *Ler* or *p35S:HA-PLP3* seeds were surface-sterilized as described (Clough and Bent, 1998). Sterile seeds were plated on GM medium (Valvekens et al., 1988) containing propyzamide (1 to 3  $\mu\text{M}$ ), taxol (0.25 to 2  $\mu\text{M}$ ), or oryzalin (25 to 150 nm), and negative controls containing the appropriate amounts of the solvent used for stock solutions (dimethyl sulfoxide). The seeds were stratified at  $4^{\circ}\text{C}$  for 2 d, and then the plates were incubated vertically at  $20^{\circ}\text{C}$ , with 16-h-light/8-h-dark cycles for 1 week. After photographing, the root length was measured using the ImageJ program (<http://rsb.info.nih.gov/ij/>).

## Yeast Two-Hybrid Screen

pGBKT7-*PLP3* and pGADT7-*PLP3* were generated by recombination between pDONR201-*PLP3a* and pDEST-GBKT7 and pDEST-GADT7 (Rossignol et al., 2007). Yeast transformation and screening were performed using standard methods (Moon et al., 1999). The yeast strain Y187 (*MAT $\alpha$* , *his3-200*, *trp1-901*, *ade2-101*, *ura3-52*, *leu2-3*, *112*, *gal4[Delta]*, *met*, *gal80 $\Delta$* , *URA3::GAL1UAS-GAL1TATA-lacZ*, *MEL1*) transformed with pGBKT7-*PLP3* was mated with the yeast strain AH109 (*MAT $\alpha$* , *trp1-901*, *m*, *leu2-3*, *112*, *ura3-52*, *his3-200*, *gal4 $\Delta$* , *gal80 $\Delta$* , *LYS::GAL1UAS-GAL1TATA-HIS3*, *MEL1 GAL2UAS-GAL2TATA-ADE2*, *URA3::MEL1UAS-MEL1TATA-lacZ*) transformed with an *Arabidopsis* inflorescence AD fusion library (from Brendan Davies, Leeds University, UK; Kieffer et al., 2006) and selected on /SD/-Leu/-Trp/-His.

## Accession Numbers

Sequence data from this article can be found in the Arabidopsis Genome Initiative or GenBank/EMBL databases under the following accession numbers. *PLP3a*, At3g50960; *PLP3b*, At5g66410;  $\beta$ -tubulin 5 (*TUB5*), At1g20010;  $\beta$ -tubulin 2 (*TUB2*), At5g62690;  $\beta$ -tubulin 3 (*TUB3*), At5g62700.1;  $\beta$ -tubulin 4 (*TUB4*), At5g44340; adenosine phosphoribosyl transferase (*APT1*), At1g27450; yeast phosphuducan-like protein 1 (*PLP1*), GenBank 851764; *Dictyostelium discoideum* phosphuducan-like protein 3 (*PhLP3*), GenBank 3385572; human thioredoxin domain containing 9 (*Txndc9*), GenBank 10190; *Caenorhabditis elegans* C05D11.3, GenBank 182257.

## Supplemental Data

The following materials are available in the online version of this article.

**Supplemental Figure 1.** Molecular Analysis of the *plp3b-1* Mutation.

**Supplemental Figure 2.** Effect of Oryzalin and Taxol on 35S: *HA-PLP3a* Seedlings Grown for 1 Week on Media Containing Oryzalin or Taxol.

**Supplemental Figure 3.** Optical Section through an Inflorescence Tip, Showing the Expression Pattern of Op:GFP Directed by the *STM<sub>pro</sub>:LhG4* Driver in the Inflorescence Meristem and Floral Meristems.

## ACKNOWLEDGMENTS

We thank Alfonso Muñoz-Gutierrez for help with experiments on the interaction between *PLP3a* and  $\beta$ -tubulin, John Doonan, Brendan Davies, Imre Somssich, Ian Moore, Tsuyoshi Nakagawa, Yuval Eshed, Phil Wigge, and Karim Sorefan for materials, and John Doonan, Peter Shaw, Michael Lenhard, Crisanto Gutierrez, and Henrik Buschmann for helpful discussions. M.M.C. received a long-term EMBO fellowship and an Intra-European Marie-Curie fellowship (MEIF-CT-2003-503985). Work in the R.S. lab is funded by the Biotechnology and Biological Sciences Research Council.

Received December 21, 2007; revised February 21, 2008; accepted March 14, 2008; published April 4, 2008.

## REFERENCES

Adams, K.L., and Wendel, J.F. (2005). Polyploidy and genome evolution in plants. *Curr. Opin. Plant Biol.* **8**: 135–141.

- Akashi, T., Izumi, K., Nagano, E., Enomoto, M., Mizuno, K., and Shibaoka, H.** (1988). Effects of propyzamide on tobacco cell microtubules in vivo and in vitro. *Plant Cell Physiol.* **29**: 1053–1062.
- Assaad, F.F., Huet, Y., Mayer, U., and Jurgens, G.** (2001). The cytokinesis gene KEULE encodes a Sec1 protein that binds the syntaxin KNOLLE. *J. Cell Biol.* **152**: 531–543.
- Bauer, P.H., Muller, S., Puzicha, M., Pippig, S., Obermaier, B., Helmreich, E.J.M., and Lohse, M.J.** (1992). Phosducin is a protein kinase-A-regulated G-protein regulator. *Nature* **358**: 73–76.
- Blaauw, M., Knol, J.C., Kortholt, A., Roelofs, J., Ruchira, Postma, M., Visser, A.J.W.G., and Van Haastert, P.J.M.** (2003). Phosducin-like proteins in *Dictyostellium discoideum*: Implications for the phosducin family of proteins. *EMBO J.* **22**: 5047–5057.
- Clough, S.J., and Bent, A.F.** (1998). Floral dip: A simplified method for *Agrobacterium*-mediated transformation of *Arabidopsis thaliana*. *Plant J.* **16**: 735–743.
- Flanary, P.L., DiBello, P.R., Estrada, P., and Dohman, H.G.** (2000). Functional analysis of Plp1 and Plp2, two homologues of phosducin in yeast. *J. Biol. Chem.* **275**: 18462–18469.
- Geissler, S., Siegers, K., and Schiebel, E.** (1998). A novel protein complex promoting formation of functional alpha- and gamma-tubulin. *EMBO J.* **17**: 952–966.
- Gomez-Mena, C., de Folter, S., Costa, M.M.R., Angenent, G.C., and Sablowski, R.** (2005). Transcriptional program controlled by the floral homeotic gene AGAMOUS during early organogenesis. *Development* **132**: 429–438.
- Gonczy, P., et al.** (2000). Functional genomic analysis of cell division in *C. elegans* using RNAi of genes on chromosome III. *Nature* **408**: 331–336.
- Grandjean, O., Vernoux, T., Laufs, P., Belcram, K., Mizukami, Y., and Traas, J.** (2004). In vivo analysis of cell division, cell growth, and differentiation at the shoot apical meristem in *Arabidopsis*. *Plant Cell* **16**: 74–87.
- Hauser, B.A., He, J.Q., Park, S.O., and Gasser, C.S.** (2000). TSO1 is a novel protein that modulates cytokinesis and cell expansion in *Arabidopsis*. *Development* **127**: 2219–2226.
- Hauser, B.A., Villanueva, J.M., and Gasser, C.S.** (1998). *Arabidopsis* TSO1 regulates directional processes in cells during floral organogenesis. *Genetics* **150**: 411–423.
- Hellens, R.P., Edwards, A.E., Leyland, N.R., Bean, S., and Mullineaux, P.M.** (2000). pGreen: A versatile and flexible binary Ti vector for *Agrobacterium*-mediated plant transformation. *Plant Mol. Biol.* **V42**: 819–832.
- Hemerly, A., Engler, Jde, A., Bergounioux, C., Van Montagu, M., Engler, G., Inze, D., and Ferreira, P.** (1995). Dominant negative mutants of the Cdc2 kinase uncouple cell division from iterative plant development. *EMBO J.* **14**: 3925–3936.
- Hugdahl, J.D., and Morejohn, L.C.** (1993). Rapid and reversible high-affinity binding of the dinitroaniline herbicide oryzalin to tubulin from *Zea mays* L. *Plant Physiol.* **102**: 725–740.
- Inze, D., and De Veylder, L.** (2006). Cell cycle regulation in plant development. *Annu. Rev. Genet.* **40**: 77–105.
- Kieffer, M., Stern, Y., Cook, H., Clerici, E., Maulbetsch, C., Laux, T., and Davies, B.** (2006). Analysis of the transcription factor WUSCHEL and its functional homologue in *Antirrhinum* reveals a potential mechanism for their roles in meristem maintenance. *Plant Cell* **18**: 560–573.
- Kirik, V., Grini, P.E., Mathur, J., Klinkhammer, I., Adler, K., Bechtold, N., Herzog, M., Bonneville, J.-M., and Hulskamp, M.** (2002b). The *Arabidopsis* TUBULIN-FOLDING COFACTOR A gene is involved in the control of the alpha/beta-tubulin monomer balance. *Plant Cell* **14**: 2265–2276.
- Kirik, V., Mathur, J., Grini, P.E., Klinkhammer, I., Adler, K., Bechtold, N., Herzog, M., Bonneville, J.M., and Hulskamp, M.** (2002a). Functional analysis of the tubulin-folding cofactor C in *Arabidopsis thaliana*. *Curr. Biol.* **12**: 1519–1523.
- Lacefield, S., Magendantz, M., and Solomon, F.** (2006). Consequences of defective tubulin folding on heterodimer levels, mitosis and spindle morphology in *Saccharomyces cerevisiae*. *Genetics* **173**: 635–646.
- Lacefield, S., and Solomon, F.** (2003). A novel step in beta-tubulin folding is important for heterodimer formation in *Saccharomyces cerevisiae*. *Genetics* **165**: 531–541.
- Liu, Z., Running, M.P., and Meyerowitz, E.M.** (1997). TSO1 functions in cell division during *Arabidopsis* flower development. *Development* **124**: 665–672.
- Lloyd, C., and Chan, J.** (2004). Microtubules and the shape of plants to come. *Nat. Rev. Mol. Cell Biol.* **5**: 13–22.
- Marc, J., Granger, C.L., Brincat, J., Fisher, D.D., Kao, T.-h., McCubbin, A.G., and Cyr, R.J.** (1998). A GFP-MAP4 reporter gene for visualizing cortical microtubule rearrangements in living epidermal cells. *Plant Cell* **10**: 1927–1940.
- Moon, Y.-H., Jung, J.-Y., Kang, H.-G., and An, G.** (1999). Identification of a rice APETALA3 homologue by yeast two-hybrid screening. *Plant Mol. Biol.* **40**: 167–177.
- Moore, I., Galweiler, L., Grosskopf, D., Schell, J., and Palme, K.** (1998). A transcription activation system for regulated gene expression in transgenic plants. *Proc. Natl. Acad. Sci. USA* **95**: 376–381.
- Muller, S., Smertenko, A., Wagner, V., Heinrich, M., Hussey, P.J., and Hauser, M.-T.** (2004). The plant microtubule-associated protein AtMAP65-3/PLE is essential for cytokinetic phragmoplast function. *Curr. Biol.* **14**: 412–417.
- Musacchio, A., and Hardwick, K.G.** (2002). The spindle checkpoint: Structural insights into dynamic signalling. *Nat. Rev. Mol. Cell Biol.* **3**: 731–741.
- Nishihama, R., Ishikawa, M., Araki, S., Soyano, T., Asada, T., and Machida, Y.** (2001). The NPK1 mitogen-activated protein kinase is a regulator of cell-plate formation in plant cytokinesis. *Genes Dev.* **15**: 352–363.
- Nishihama, R., Soyano, T., Ishikawa, M., Araki, S., Tanaka, H., Asada, T., Irie, K., Ito, M., Terada, M., Banno, H., Yamazaki, Y., and Machida, Y.** (2002). Expansion of the cell plate in plant cytokinesis requires a kinesin-like protein/MAPKKK complex. *Cell* **109**: 87–99.
- Ogawa, S., Matsubayashi, Y., and Nishida, E.** (2004). An evolutionarily conserved gene required for proper microtubule architecture in *Caenorhabditis elegans*. *Genes Cells* **9**: 83–93.
- Rieder, C.L., and Maiato, H.** (2004). Stuck in division or passing through: what happens when cells cannot satisfy the spindle assembly checkpoint. *Dev. Cell* **7**: 637–651.
- Rosignol, P., Collier, S., Bush, M., Shaw, P., and Doonan, J.H.** (2007). *Arabidopsis* POT1A interacts with TERT-V(18), an N-terminal splicing variant of telomerase. *J. Cell Sci.* **120**: 3678–3687.
- Schiff, P.B., Fant, J., and Horwitz, S.B.** (1979). Promotion of microtubule assembly in vitro by taxol. *Nature* **277**: 665–667.
- Sieburth, L.E., and Meyerowitz, E.M.** (1997). Molecular dissection of the AGAMOUS control region shows that cis elements for spatial regulation are located intragenically. *Plant Cell* **9**: 355–365.
- Sollner, R., Glasser, G., Wanner, G., Somerville, C.R., Jurgens, G., and Assaad, F.F.** (2002). Cytokinesis-defective mutants of *Arabidopsis*. *Plant Physiol.* **129**: 678–690.
- Song, J., Leung, T., Ehler, L.K., Wang, C., and Liu, Z.** (2000). Regulation of meristem organization and cell division by TSO1, an *Arabidopsis* gene with cysteine-rich repeats. *Development* **127**: 2207–2217.
- Srayko, M., Kaya, A., Stamford, J., and Hyman, A.A.** (2005). Identification and characterization of factors required for microtubule growth and nucleation in the early *C. elegans* embryo. *Dev. Cell* **9**: 223–236.



- Steinborn, K., Maulbetsch, C., Priester, B., Trautmann, S., Pacher, T., Geiges, B., Kuttner, F., Lepiniec, L., Stierhof, Y.-D., Schwarz, H., Jurgens, G., and Mayer, U. (2002). The Arabidopsis PILZ group genes encode tubulin-folding cofactor orthologs required for cell division but not cell growth. *Genes Dev.* **16**: 959–971.
- Stirling, P.C., Cuellar, J., Alfaro, G.A., El Khadali, F., Beh, C.T., Valpuesta, J.M., Melki, R., and Leroux, M.R. (2006). PhLP3 modulates CCT-mediated actin and tubulin folding via ternary complexes with substrates. *J. Biol. Chem.* **281**: 7012–7021.
- Strompen, G., El Kasmi, F., Richter, S., Lukowitz, W., Assaad, F.F., Jurgens, G., and Mayer, U. (2002). The Arabidopsis HINKEL gene encodes a kinesin-related protein involved in cytokinesis and is expressed in a cell cycle-dependent manner. *Curr. Biol.* **12**: 153–158.
- Sugimoto-Shirasu, K., and Roberts, K. (2003). “Big it up”: Endoreduplication and cell-size control in plants. *Curr. Opin. Plant Biol.* **6**: 544–553.
- Sugimoto-Shirasu, K., Stacey, N.J., Corsar, J., Roberts, K., and McCann, M.C. (2002). DNA topoisomerase VI is essential for endoreduplication in Arabidopsis. *Curr. Biol.* **12**: 1782–1786.
- Szymanski, D. (2002). Tubulin folding cofactors: Half a dozen for a dimer. *Curr. Biol.* **12**: R767.
- Till, B.J., et al. (2003). Large-scale discovery of induced point mutations with high-throughput TILLING. *Genome Res.* **13**: 524–530.
- Tong, A.H.Y., et al. (2004). Global mapping of the yeast genetic interaction network. *Science* **303**: 808–813.
- Torres-Ruiz, R.A., and Jurgens, G. (1994). Mutations in the *fass* gene uncouple pattern-formation and morphogenesis in Arabidopsis development. *Development* **120**: 2967–2978.
- Traas, J., Bellini, C., Nacry, P., Kronenberger, J., Bouchez, D., and Caboche, M. (1995). Normal differentiation patterns in plants lacking microtubular preprophase bands. *Nature* **375**: 676–677.
- Tzafrir, I., McElver, J.A., Liu, C.-m., Yang, L.J., Wu, J.Q., Martinez, A., Patton, D.A., and Meinke, D.W. (2002). Diversity of TITAN functions in Arabidopsis seed development. *Plant Physiol.* **128**: 38–51.
- Ueda, K., Matsuyama, T., and Hashimoto, T. (1999). Visualization of microtubules in living cells of transgenic Arabidopsis thaliana. *Protoplasma* **206**: 201–206.
- Vainberg, I.E., Lewis, S.A., Rommelaere, H., Ampe, C., Vandekerckhove, J., Klein, H.L., and Cowan, N.J. (1998). Prefoldin, a chaperone that delivers unfolded proteins to cytosolic chaperonin. *Cell* **93**: 863–873.
- Valvekens, D., Vanmontagu, M., and Vanlijsebettens, M. (1988). *Agrobacterium tumefaciens*-mediated transformation of Arabidopsis thaliana root explants by using kanamycin selection. *Proc. Natl. Acad. Sci. USA* **85**: 5536–5540.
- Waizenegger, I., Lukowitz, W., Assaad, F., Schwarz, H., Jurgens, G., and Mayer, U. (2000). The Arabidopsis KNOLLE and KEULE genes interact to promote vesicle fusion during cytokinesis. *Curr. Biol.* **10**: 1371–1374.
- Wang, Y.-S., Motes, C.M., Mohamalawari, D.R., and Blancaflor, E.B. (2004). Green fluorescent protein fusions to Arabidopsis fimbrin 1 for spatio-temporal imaging of F-actin dynamics in roots. *Cell Motil. Cytoskeleton* **59**: 79–93.
- Weaver, B.A.A., and Cleveland, D.W. (2005). Decoding the links between mitosis, cancer, and chemotherapy: The mitotic checkpoint, adaptation, and cell death. *Cancer Cell* **8**: 7–12.
- Yanai, O., Shani, E., Dolezal, K., Tarkowski, P., Sablowski, R., Sandberg, G., Samach, A., and Ori, N. (2005). Arabidopsis KNOX1 proteins activate cytokinin biosynthesis. *Curr. Biol.* **15**: 1566–1571.